JOURNAL OF SPACECRAFT AND ROCKETS
Vol. 46, No. 2, March–April 2009

Saturn Impact Trajectories for Cassini End-of-Mission

Chit Hong Yam,* Diane Craig Davis,† James M. Longuski,‡ and Kathleen C. Howell§
Purdue University, West Lafayette, Indiana 47907-2045
and
Brent Buffington¶
Jet Propulsion Laboratory, California Institute of Technology, Pasadena, California 91109-8099

DOI: 10.2514/1.38760

Potential end-of-mission scenarios to be considered for the Cassini spacecraft must satisfy planetary quarantine requirements designed to prevent contamination of a pristine environment, which could include Titan and the other Saturnian moons. One assumed acceptable option for safe disposal of the spacecraft includes Saturn impact trajectories. Two classes of impact trajectories are investigated: short-period orbits characterized by periods of 6–10 days and long-period orbits with periods greater than 850 days. To impact Saturn with short-period orbits, a series of successive Titan flybys is required to increase inclination and decrease periapsis to within Saturn's atmosphere, while simultaneously avoiding the rings and mitigating ΔV expenditures. To ensure that the spacecraft is not prematurely damaged by material in the rings, Tisserand graphs are employed to determine when the ring-plane crossing distance is within the F–G ring gap: the necessary geometry for the penultimate transfer. For long-period impact trajectories, solar gravity is exploited to significantly lower periapsis. Depending on the size and orientation of the long-period orbit, a maneuver (<50 m/s) at apoapsis must be added to ensure impact. For sufficiently large orbits with favorable characteristics, solar gravity alone drops the spacecraft's periapsis into Saturn's atmosphere. No maneuver is necessary after the final Titan flyby, providing an attractive "flyby-and-forget" option.

Nomenclature

a	=	semimajor axis, km or R_S
e	=	eccentricity
h	=	specific angular momentum, km^2/s
h_p	=	flyby altitude, km
i_{rel}	=	inclination relative to the gravity-assist body's orbit, deg
J_2	=	Saturn's oblateness coefficient
m	=	number of gravity-assist body orbits about the central body
n	=	number of spacecraft orbits about the central body
p	=	semilatus rectum, km or R_S
R_S	=	Saturn's radius, km ($R_S = 60,268$ km)
R_T	=	Titan's radius, km ($R_T = 2575$ km)
$\mathbf{r}$	=	position vector from the central body, km or R_S
r	=	radial distance from center of Saturn to spacecraft, km or R_S
r_a	=	radius of apoapsis from central body, km or R_S
r_{enc}	=	radial distance of encounter from central body, km or R_S
r_p	=	radius of periapsis from central body, km or R_S
r_{vac}	=	radial distance of vacant node from central body, km or R_S
T	=	orbital period, day
$\mathbf{V}$	=	velocity vector relative to the central body, km/s
$\mathbf{V}_\infty$	=	hyperbolic excess velocity vector, km/s
v	=	velocity magnitude relative to the central body, km/s
v_∞	=	hyperbolic excess velocity magnitude, km/s
α	=	pump angle, deg
γ	=	flight-path angle, deg
ΔV	=	change in velocity magnitude, km/s
δ	=	flyby bending angle, deg
θ	=	flyby B-plane angle, deg
κ	=	crank angle, deg
μ	=	gravitational parameter, km^3/s^2
ϕ	=	orientation of the spacecraft orbit relative to the sun-Saturn line, deg

Subscripts

ga	=	quantity for the gravity-assist body
sc	=	quantity for the spacecraft

Received 29 May 2008; revision received 21 December 2008; accepted for publication 26 December 2008.

*Ph.D. Candidate, School of Aeronautics and Astronautics, 701 West Stadium Avenue; currently Research Fellow, Advanced Concepts Team, European Space Research and Technology Centre, ESA, Keplerlaan 1, 2201 AZ Noordwijk, The Netherlands; chithongyam@gmail.com.

†Ph.D. Candidate, School of Aeronautics and Astronautics, 701 West Stadium Avenue; decraig@purdue.edu. Student Member AIAA.

‡Professor, School of Aeronautics and Astronautics, 701 West Stadium Avenue; longuski@purdue.edu. Associate Fellow AIAA.

§Hsu Lo Professor of Aeronautical and Astronautical Engineering, School of Aeronautics and Astronautics, 701 West Stadium Avenue; howell@purdue.edu. Associate Fellow AIAA.

¶Member of Engineering Staff, Guidance, Navigation, and Control Section, 4800 Oak Grove Drive; Brent.Buffington@jpl.nasa.gov. Member AIAA.

Introduction

AFTER extraordinary success in exploring the Saturnian system [1], the future of the Cassini spacecraft must ultimately be decided. Potential end-of-mission scenarios must satisfy planetary quarantine requirements put in place to prevent contamination of sensitive environments, which could include Titan and other Saturnian moons.** Two scenarios are believed to satisfy these requirements: effective impact with a gas giant, as in the case of the Galileo mission [3], or guarantee (to some acceptable statistical certainty) no possible impact for at least 500 years of flight. Several possible long-term orbits have been proposed, including orbits that remain within the Saturnian system [4,5] and trajectories that escape

**The NASA Planetary Protection Office currently considers Titan a category II body [2]; all other Saturnian satellites do not have a planetary protection status. However, based on discoveries by the Cassini–Huygens mission, the level of planetary protection for Titan (and potentially other Saturnian satellites, most notably Enceladus) could be elevated.

from Saturn to impact on Jupiter, Uranus, or Neptune [6]. In this work, Saturn impact orbits are considered. Entry into Saturn's atmosphere would bring the Cassini mission to an end, ensuring no possible future impact with a sensitive environment.

Because the Cassini spacecraft is already flying its extended mission in orbit about Saturn, the initial conditions for the final end-of-life stage of the mission are constrained. In addition, the ΔV available for maneuvers is limited by the amount of propellant remaining on board. It is therefore a challenge to place the spacecraft on an impact trajectory. Given a state vector at the conclusion of the extended mission, two strategies for maneuvering the spacecraft onto an impact trajectory are investigated: 1) using short-period orbits with Titan gravity assists, and 2) exploiting solar gravity with a long-period orbit.

For short-period orbits with periods of 6–10 days, gravity assists are used to drop the periapsis into Saturn's atmosphere. Titan, being the most massive moon of Saturn, serves as the most effective gravity-assist body in the Saturnian system. Since its arrival at Saturn in July 2004, Cassini has performed over 40 flybys at Titan in its primary mission, which was completed in July 2008 [7–11]. Up to a total of 70 Titan flybys have been planned for its extended mission through June 2010 [12]. For tour design, Titan-to-Titan transfers pump the energy up (or down) and crank the inclination (as described in [9,10,13]) to achieve the desired conditions. One challenge in designing a short-period impact trajectory is the constraint involving crossings of Saturn's ring plane. Although one of the science objectives of the Cassini/Huygens mission is to observe the structure and dynamic behavior of Saturn's rings [14], the rings pose a hazard, as debris from the rings can damage the spacecraft. Passage through the ring plane is considered safe as long as the node crossing occurs either within a gap in the rings or beyond the G ring (i.e., $r > 2.92\ R_S$). For example, upon arrival at Saturn in July 2004, Cassini passed through the gap between the G ring and the F ring [7–9]. For short-period impact trajectories, a new application of the Tisserand graph is used to find potential orbits that cross the ring plane in the safe F–G ring gap.

The second strategy for placing the spacecraft on a Saturn impact trajectory involves large orbits with periods greater than 850 days. The effect of solar gravity can be significant on such large orbits, and when the trajectory is oriented appropriately with respect to the sun, solar gravity causes a substantial decrease in periapse radius. Combined with a maneuver at apoapsis, solar gravity can be sufficient to drop the spacecraft into Saturn's atmosphere. A factor to consider, however, is the time between the final Titan flyby and the apoapse maneuver. Already nearing the end of its lifetime, the spacecraft must be able to perform an effective maneuver. However, an orbit of sufficient size and appropriate orientation, inclination, and starting periapse radius will impact Saturn without requiring a maneuver at apoapsis. Because no maneuver is necessary after the final Titan flyby, these orbits present an attractive flyby-and-forget option.

In this work, the steps in developing each strategy are detailed. Results that yield a Saturn impact are summarized, and insights into this end-of-mission approach are offered. Confirmation of the results is obtained via transition of sample trajectories to a higher-fidelity model.

Background of the Cassini–Huygens Mission

After the encounters at Saturn by Pioneer 11 and Voyagers 1 and 2, plans for a Saturn orbiter began in 1982, which later became the Cassini–Huygens mission [15,16]. Miner [17], Matson et al. [18], and Cuzzi et al. [19] describe the primary science objectives, which include observations of Saturn, the rings, the magnetosphere, Titan, and other satellites. Some important discoveries from the mission are reported in [20,21] on finding water vapor plumes on Enceladus, confirming the presence of lakes of liquid methane on Titan [22], and, in [23,24], announcing the detection of new moons.

After seven years of interplanetary cruise [25], the Cassini orbiter was inserted into orbit about Saturn in July 2004 [1], whereas the Huygens probe was delivered to the surface of Titan in January 2005 [26,27]. Goodson et al. [28], Standley [29], and Wagner et al. [30] describe the engineering operations and maneuver experience during the mission. The Cassini primary mission ended in July 2008 [11], with an extended mission planned until June 2010 [12].

Analysis

In this section, the technique of gravity assist is reviewed. Based on the work presented in [31–33], the Tisserand criterion for a gravity-assist body on an elliptic orbit is derived. Expressions are presented for relationships between the orbital elements about the central body, which aid the design of gravity-assist impact trajectories. Effects of solar gravity are included.

Touring in the Saturnian System

For short-period impact trajectories, a two-body patched-conic model [34,35] is employed. Such a model assumes that the spacecraft is in a two-body conic orbit about the central body (e.g., Saturn). A gravity-assist flyby of a satellite (e.g., Titan) is regarded as an instantaneous change in velocity relative to the central body (i.e., zero sphere of influence). The patched-conic analysis provides a preliminary design of gravity-assist trajectories, which builds a sequence of Keplerian orbits as an initial guess for numerical integration and optimization in a full-force model.

To reach a desired final condition (e.g., Saturn impact), a series of Titan-to-Titan transfers (i.e., a tour) is used to control the orbital parameters. Successive Titan flybys can be assured when the spacecraft enters a resonant orbit: the ratio of the spacecraft's period to the satellite's period is a rational number (i.e., fraction of integers). Let m be the number of gravity-assist body (Titan) orbits about the central body and n be the number of spacecraft orbits (before the next Titan encounter) about the central body. For an m:n resonance orbit (where m and n are integers), the period of the spacecraft T_{sc} can be found as

$$T_{\text{sc}} = (m/n)T_{\text{ga}} \tag{1}$$

where T_{ga} is the period of the gravity-assist body, Titan. The semimajor axis a_{sc} and the period of the spacecraft T_{sc} are related by

$$a_{\text{sc}}^3 = \mu_{\text{cb}}(T_{\text{sc}}/2\pi)^2 \tag{2}$$

where μ_{cb} is the gravitational parameter of the central body, Saturn. Period (and size) of the spacecraft orbit can be increased (or decreased) via orbit pumping [36], whereas orbit cranking changes the inclination of the spacecraft orbit relative to the central body [13].

$\mathbf{V}_\infty$ in Terms of Orbital Parameters

At the moment of encountering the gravity-assist (GA) body, the position (from the central body) of the spacecraft and the position of the gravity-assist body are modeled as equal, that is,

$$\mathbf{r}_{\mathbf{sc}} = \mathbf{r}_{\mathbf{ga}} \tag{3}$$

$$r_{\text{enc}} = \|\mathbf{r}_{\mathbf{sc}}\| = \|\mathbf{r}_{\mathbf{ga}}\| \tag{4}$$

where $\mathbf{r}_{\mathbf{sc}}$ and $\mathbf{r}_{\mathbf{ga}}$ are the position vectors of the spacecraft and the GA body (Titan), respectively, and bold denotes a vector. The hyperbolic excess velocity $\mathbf{V}_\infty$ is the velocity vector of the spacecraft relative to the GA body before or after an encounter. The $\mathbf{V}_\infty$ vector is also the difference between the velocity of the spacecraft $\mathbf{V}_{\mathbf{sc}}$ and the velocity of the GA body $\mathbf{V}_{\mathbf{ga}}$, that is,

$$\mathbf{V}_\infty = \mathbf{V}_{\mathbf{sc}} - \mathbf{V}_{\mathbf{ga}} \tag{5}$$

Following an approach similar to that of Strange and Sims [31], the velocities $\mathbf{V}_{\mathbf{sc}}$ and $\mathbf{V}_{\mathbf{ga}}$ can be written in a coordinate frame tied to the orbit plane of the GA body, using unit vectors $\hat{\mathbf{p}}_1 - \hat{\mathbf{p}}_2 - \hat{\mathbf{p}}_3$, as

$$\mathbf{V}_{\mathbf{sc}} = v_{\text{sc}}(\sin\gamma_{\text{sc}}\hat{\mathbf{p}}_1 + \cos\gamma_{\text{sc}}\cos i_{\text{rel}}\hat{\mathbf{p}}_2 + \cos\gamma_{\text{sc}}\sin i_{\text{rel}}\hat{\mathbf{p}}_3) \tag{6}$$

$$\mathbf{V_{ga}} = v_{ga}(\sin\gamma_{ga}\hat{\mathbf{p}}_1 + \cos\gamma_{ga}\hat{\mathbf{p}}_2) \tag{7}$$

$$\hat{\mathbf{p}}_1 = \mathbf{r_{ga}}/\|\mathbf{r_{ga}}\| \qquad \hat{\mathbf{p}}_3 = \mathbf{r_{ga}} \times \mathbf{V_{ga}}/\|\mathbf{r_{ga}} \times \mathbf{V_{ga}}\| \qquad \hat{\mathbf{p}}_2 = \hat{\mathbf{p}}_3 \times \hat{\mathbf{p}}_1 \tag{8}$$

where γ_{sc} and γ_{ga} are the flight-path angles of the spacecraft and the GA body, respectively. Instead of using Saturn's equator, the GA body's (i.e., Titan's) orbit plane is used as the reference plane (similar to the approach of Strange [32]). Note that the angle i_{rel} in Eq. (6) is the inclination of the spacecraft orbit relative to the GA body's orbit plane (i.e., the angle between the angular momentum vectors of the spacecraft orbit and the GA body's orbit), where i_{rel} ranges from -180 to 180 deg. Positive i_{rel} indicates that the encounter is at the ascending node (relative to the GA body's orbit), that is, the spacecraft is approaching from below the reference plane; and negative i_{rel} indicates that the encounter is at the descending node, that is, the spacecraft is approaching from above the GA's orbit plane. Substituting Eqs. (6) and (7) into Eq. (5) gives

$$\mathbf{V}_\infty = (v_{sc}\sin\gamma_{sc} - v_{ga}\sin\gamma_{ga})\hat{\mathbf{p}}_1 + (v_{sc}\cos\gamma_{sc}\cos i_{rel} - v_{ga}\cos\gamma_{ga})\hat{\mathbf{p}}_2 + (v_{sc}\cos\gamma_{sc}\sin i_{rel})\hat{\mathbf{p}}_3 \tag{9}$$

A dot product of $\mathbf{V}_\infty$ with itself in Eq. (9) yields an expression of the magnitude (as provided in [31,32]):

$$\mathbf{V}_\infty \cdot \mathbf{V}_\infty = v_\infty^2 = v_{sc}^2 + v_{ga}^2 - 2v_{sc}v_{ga}(\sin\gamma_{sc}\sin\gamma_{ga} + \cos\gamma_{sc}\cos\gamma_{ga}\cos i_{rel}) \tag{10}$$

Because a gravity assist changes the direction, but not the magnitude of the $\mathbf{V}_\infty$, Eq. (10) provides a relationship between the spacecraft orbital parameters: v_{sc}, γ_{sc}, and i_{rel} for a given set of GA orbital parameters v_{ga} and γ_{ga}. For Titan-to-Titan resonant transfers, in theory, the spacecraft encounters Titan at the same inertial location (i.e., $\mathbf{r_{ga}}$ and $\mathbf{V_{ga}}$ do not change) and the v-infinity magnitude ($v_\infty = \|\mathbf{V}_\infty\|$) remains constant. In practice, perturbations (e.g., solar and J_2) may shift the return encounter location of Titan. The velocity relative to the central body and the flight-path angle can be written as

$$v^2 = \mu(2/r - 1/a) \tag{11}$$

$$\cos\gamma = h/(rv) = \sqrt{\mu a(1-e^2)}/(rv) = \sqrt{\mu p}/(rv) \tag{12}$$

$$\sin\gamma = \pm\sqrt{1-\cos^2(\gamma)} = \pm\sqrt{r^2v^2 - \mu p}/(rv) \tag{13}$$

where $p = a(1-e^2)$ is the semilatus rectum. The $\pm$ sign in Eq. (13) corresponds to outbound orbits (+) and inbound orbits (−), respectively. Equation (10) can be rewritten in terms of the semimajor axis and the semilatus rectum by substitution of Eqs. (11–13):

$$4 - v_\infty^2/(\mu_{cb}/r_{enc}) = r_{enc}/a_{sc} + r_{enc}/a_{ga} + 2\left[\left(\sqrt{p_{sc}/r_{enc}}\right)\left(\sqrt{p_{ga}/r_{enc}}\right)\cos i_{rel} \pm \left(\sqrt{2 - r_{enc}/a_{sc} - p_{sc}/r_{enc}}\right)\left(\sqrt{2 - r_{enc}/a_{ga} - p_{ga}/r_{enc}}\right)\right] \tag{14}$$

where a_{sc} and a_{ga} are the semimajor axes of the spacecraft orbit and the GA body's orbit, and p_{sc} and p_{ga} are the semilatus rectums of the spacecraft orbit and the GA body's orbit. The $\pm$ sign in Eq. (14) corresponds to the combinations of outbound/inbound orbits of the spacecraft and the GA body: positive (+) when both spacecraft and GA body are outbound or when both are inbound (i.e., product of the flight-path angles $\gamma_{sc}\gamma_{ga} > 0$); negative (−) when one is outbound and one is inbound (i.e., product of the flight-path angles $\gamma_{sc}\gamma_{ga} < 0$). Note that Eq. (14) is the Tisserand criterion [37–39] for an elliptic GA body's orbit. For a circular GA body's orbit, $a_{ga} = p_{ga} = r_{enc}$ yields (as given by Strange and Longuski [39])

$$3 - v_\infty^2/(\mu_{cb}/r_{enc}) = r_{enc}/a_{sc} + 2\cos i_{rel}\sqrt{p_{sc}/r_{enc}} \tag{15}$$

Equation (14) [or Eq. (15)] provides an invariant relationship between the semimajor axis a_{sc}, the semilatus rectum p_{sc}, and the inclination i_{rel} for gravity-assist trajectories. In designing the Europa orbiter mission, Heaton et al. [40] assume circular orbits for the GA bodies (Galilean satellites) and coplanar orbits for the GA bodies and the spacecraft. For designing Saturn impact trajectories, however, the eccentricity of Titan (0.0288) cannot be neglected (as will be shown later) and therefore Eq. (14) is used instead of Eq. (15).

$\mathbf{V}_\infty$ in Terms of Pump and Crank Angles

Equation (9) offers a way to express the $\mathbf{V}_\infty$ in terms of the velocity, the flight-path angle, and the inclination (v_{sc}, γ_{sc}, and i_{rel}). The $\mathbf{V}_\infty$ can also be parameterized in terms of the pump angle α and the crank angle κ as

$$\mathbf{V}_\infty = v_\infty(\sin\alpha\cos\kappa\hat{\mathbf{q}}_1 + \cos\alpha\hat{\mathbf{q}}_2 - \sin\alpha\sin\kappa\hat{\mathbf{q}}_3) \tag{16}$$

where the unit vectors $\hat{\mathbf{q}}_1 - \hat{\mathbf{q}}_2 - \hat{\mathbf{q}}_3$ are given by

$$\hat{\mathbf{q}}_2 = \mathbf{V_{ga}}/\|\mathbf{V_{ga}}\| \qquad \hat{\mathbf{q}}_3 = \mathbf{r_{ga}} \times \mathbf{V_{ga}}/\|\mathbf{r_{ga}} \times \mathbf{V_{ga}}\| \qquad \hat{\mathbf{q}}_1 = \hat{\mathbf{q}}_2 \times \hat{\mathbf{q}}_3 \tag{17}$$

The pump angle α is the angle between the v-infinity vector and the velocity of the GA body with respect to the central body (see Fig. 1). The magnitude of the spacecraft velocity can be found by applying the law of cosines on the $\mathbf{V_{ga}}$-$\mathbf{V}_\infty$-$\mathbf{V_{sc}}$ triangle:

$$v_{sc}^2 = v_{ga}^2 + v_\infty^2 + 2v_\infty v_{ga}\cos\alpha \tag{18}$$

The pump angle α can range from 0 to 180 deg. It is directly related to the spacecraft speed v_{sc} relative to the central body, and hence the orbital energy and semimajor axis. Less energetic orbits have larger pump angles and vice versa. For given v_{ga} and v_∞, $\alpha = 0$ deg and $\alpha = 180$ deg represent the most energetic and the least energetic orbits possible (respectively) for encountering the GA body.

The crank angle κ is an angle measured in the plane perpendicular to the GA body's orbit plane (see Fig. 1), where the reference line for zero κ is $\hat{\mathbf{q}}_1$ (where $\hat{\mathbf{q}}_1 = \hat{\mathbf{r}}_{ga}$ when GA body's orbit is circular). (In Fig. 1, the illustration shows a case where $\kappa > 180$ deg for aesthetic reasons.) The crank angle κ can range from -180 to 180 deg. It measures how "inclined" the $\mathbf{V}_\infty$ is relative to the GA body's orbit plane. When $\kappa = 0$ or 180 deg, the $\mathbf{V_{ga}}$-$\mathbf{V}_\infty$-$\mathbf{V_{sc}}$ triangle lies on the

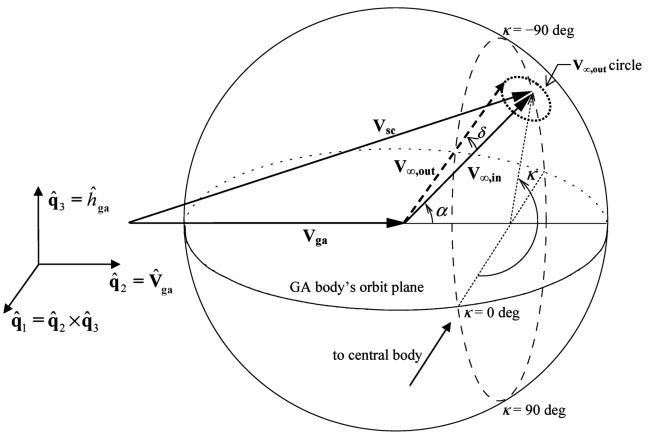

Fig. 1 V_∞ sphere (after Strange et al. [33], Rinderle [45], and Russell and Ocampo [54]).

GA body's orbit plane, which means the spacecraft and the GA body share the same orbit plane (i.e., $i_{\text{rel}} = 0$ or 180 deg). The quadrant of κ can also provide information of the encounter type at the GA body: $0 < \kappa < 180$ deg means the encounter is descending (i.e., spacecraft approaching the GA body from above the reference plane); $-180 < \kappa < 0$ deg means the encounter is ascending; $-90 < \kappa < 90$ deg means encounter is outbound (i.e., spacecraft is approaching its apoapsis); $90 < \kappa < 180$ deg or $-180 < \kappa < -90$ deg means inbound encounter (i.e., spacecraft is approaching its periapsis).

Equations (9) and (16) are expressions of the $\mathbf{V}_\infty$ in terms of two sets of parameters (α, κ and $v_{\text{sc}}, \gamma_{\text{sc}}, i_{\text{rel}}$). A relationship between these two sets of parameters can be useful for the design of gravity-assist trajectories. The unit vectors $\hat{\mathbf{q}}_1 - \hat{\mathbf{q}}_2 - \hat{\mathbf{q}}_3$ can be written in terms of $\hat{\mathbf{p}}_1 - \hat{\mathbf{p}}_2 - \hat{\mathbf{p}}_3$ as

$$\hat{\mathbf{q}}_1 = \cos\gamma_{\text{ga}}\hat{\mathbf{p}}_1 - \sin\gamma_{\text{ga}}\hat{\mathbf{p}}_2 \qquad \hat{\mathbf{q}}_2 = \sin\gamma_{\text{ga}}\hat{\mathbf{p}}_1 + \cos\gamma_{\text{ga}}\hat{\mathbf{p}}_2 \qquad \hat{\mathbf{q}}_3 = \hat{\mathbf{p}}_3 \tag{19}$$

Substituting Eq. (19) into Eq. (16) and comparing coefficients of $\hat{\mathbf{p}}_1$, $\hat{\mathbf{p}}_2$, and $\hat{\mathbf{p}}_3$ with Eq. (9) yields

$$v_{\text{sc}}\sin\gamma_{\text{sc}} = v_\infty(\cos\alpha\sin\gamma_{\text{ga}} + \sin\alpha\cos\kappa\cos\gamma_{\text{ga}}) + v_{\text{ga}}\sin\gamma_{\text{ga}} \tag{20}$$

$$v_{\text{sc}}\cos\gamma_{\text{sc}}\cos i_{\text{rel}} = v_\infty(\cos\alpha\cos\gamma_{\text{ga}} - \sin\alpha\cos\kappa\sin\gamma_{\text{ga}}) + v_{\text{ga}}\cos\gamma_{\text{ga}} \tag{21}$$

$$v_{\text{sc}}\cos\gamma_{\text{sc}}\sin i_{\text{rel}} = -v_\infty\sin\alpha\sin\kappa \tag{22}$$

For a given v_∞ magnitude and given GA body's parameters (v_{ga} and γ_{ga}), Eqs. (18) and (20–22) can be used to solve for spacecraft orbital parameters (v_{sc}, γ_{sc}, and i_{rel}) from pump and crank angles (α and κ), and vice versa (pump and crank angles can be determined from spacecraft orbital parameters).

Bending of $\mathbf{V}_\infty$ After Flyby

A gravity-assist flyby rotates $\mathbf{V}_\infty$ while keeping the magnitude v_∞ constant. That is, a planetary satellite (e.g., Titan) encounter *bends* the incoming (preflyby) v-infinity vector ($\mathbf{V}_{\infty,\mathbf{in}}$) into the outgoing (postflyby) v-infinity vector ($\mathbf{V}_{\infty,\mathbf{out}}$). The angle between $\mathbf{V}_{\infty,\mathbf{in}}$ and $\mathbf{V}_{\infty,\mathbf{out}}$ is referred to as the bending angle δ, given by

$$\sin(\delta/2) = 1/[1 + (h_p + R_{\text{ga}})v_\infty^2/\mu_{\text{ga}}] \tag{23}$$

where h_p is the flyby altitude, R_{ga} is the radius of the gravity-assist body, and μ_{ga} is the gravitational parameter of the gravity-assist body, Titan. From Eq. (23), it is apparent that the bending angle only depends on the flyby altitude h_p (because other quantities are constant during flyby). A lower flyby altitude produces a larger bending of the $\mathbf{V}_\infty$ (and hence a bigger change in orbital elements about the central body). For a given incoming v-infinity vector $\mathbf{V}_{\infty,\mathbf{in}}$ and flyby altitude h_p (or bending angle δ), the outgoing v-infinity vector $\mathbf{V}_{\infty,\mathbf{out}}$ is given as

$$\mathbf{V}_{\infty,\text{out}} = v_\infty(-\sin\delta\cos\theta\hat{\mathbf{b}}_1 - \sin\delta\sin\theta\hat{\mathbf{b}}_2 + \cos\delta\hat{\mathbf{b}}_3) \tag{24}$$

$$\hat{\mathbf{b}}_3 = \mathbf{V}_{\infty,\text{in}}/\|\mathbf{V}_{\infty,\text{in}}\| \qquad \hat{\mathbf{b}}_1 = \hat{\mathbf{b}}_3 \times \hat{\mathbf{n}}/\|\hat{\mathbf{b}}_3 \times \hat{\mathbf{n}}\| \qquad \hat{\mathbf{b}}_2 = \hat{\mathbf{b}}_3 \times \hat{\mathbf{b}}_1 \tag{25}$$

where θ is the flyby B-plane angle [41] ($-180 < \theta \leq 180$ deg), $\hat{\mathbf{n}}$ is the unit pole vector $= 0\hat{x} + 0\hat{y} + \hat{z}$, and $\hat{x}, \hat{y}, \hat{z}$ are the Cartesian unit vectors of the reference frame (e.g., Saturn equator and equinox of epoch).

Figure 1 illustrates a $\mathbf{V}_\infty$ sphere with radius equal to the magnitude of the v-infinity vector v_∞. The pump and crank angles can be defined (as described previously) for any $\mathbf{V}_\infty$, incoming or outgoing. (The pump and crank angles α and κ in Fig. 1 refer to $\mathbf{V}_{\infty,\mathbf{in}}$.) A constant bending angle δ with a sampling of the B-plane angle θ from -180 to 180 deg creates a circular locus on the v-infinity sphere for the outgoing v-infinity vector $\mathbf{V}_{\infty,\mathbf{out}}$. Each point on the $\mathbf{V}_{\infty,\mathbf{out}}$ circle represents a different postflyby orbit about the central body and a different set of postflyby pump and crank angles. Once the pump and crank angles for $\mathbf{V}_{\infty,\mathbf{out}}$ [from Eqs. (16) and (24)] are determined, orbital elements after the flyby can be solved through Eqs. (18) and (20–22). Also, the area inside the $\mathbf{V}_{\infty,\mathbf{out}}$ circle corresponds to flybys with a bending angle smaller than δ (or flyby higher than an altitude of h_p). Thus, the $\mathbf{V}_{\infty,\mathbf{out}}$ circle provides a way to predict the family of outgoing orbits after a single flyby with a constraint on the flyby altitude (e.g., $h_p \geq 1000$ km at Titan).

Vacant Node Crossing Distance and Rings

The ascending and descending nodes are the locations where the spacecraft's orbit intersects a reference plane. In the patched-conic analysis employed in this paper, the GA body's orbit plane (Titan's orbit) is used as the reference plane, which constrains the GA body's encounter to be at one of the nodes. [Titan's orbit is slightly inclined (0.365 deg) relative to Saturn's equator, the ring plane.] Figure 2 shows a typical Cassini orbit about Saturn, where the Titan encounter is at the descending node (i.e., the spacecraft approaches Titan from above the reference plane). Besides the Titan encounter, the spacecraft also intersects the reference plane at the ascending node where the GA body is not present. Such a node crossing is referred to as a vacant node [32]. The distance from Saturn's center to the vacant

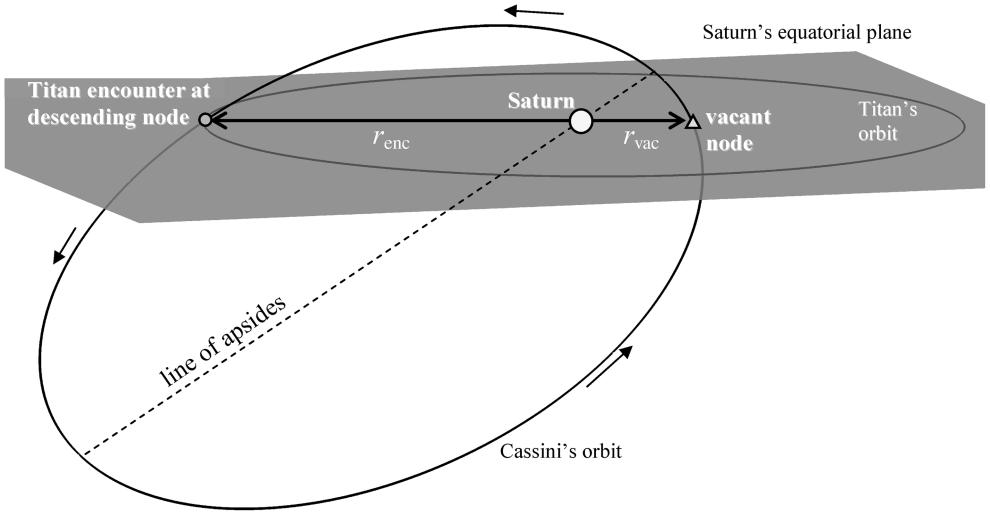

Fig. 2 Titan encounter and the vacant node.

node is defined as r_{vac}. The vacant node crossing distance r_{vac} can be written in terms of the semilatus rectum p_{sc} and the encounter distance r_{enc} as

$$r_{vac} = \frac{1}{2/p_{sc} - 1/r_{enc}} \tag{26}$$

(See Strange [32] for derivation.) To minimize the likelihood of impact damage to the spacecraft, the node crossings should occur either within a gap between the F and G rings or beyond the G ring, that is, the node crossing must satisfy the following criteria:

$$2.347\ R_S < r_{vac} < 2.730\ R_S \quad \text{or} \quad r_{vac} > 2.917\ R_S \tag{27}$$

(For descriptions of Saturn's ring system, see Cuzzi et al. [19]) The spacecraft is assumed to be able to safely pass through the ring plane as long as its node crossing satisfies Eq. (27).

For Titan-to-Titan resonant transfers, the encounter distance r_{enc} is constant (in theory) and r_{vac} only depends on the semilatus rectum p_{sc}. Expressions relating p_{sc} and the pump and crank angles can be found by summing the squares of Eqs. (21) and (22):

$$\begin{aligned}&(v_{sc}\cos\gamma_{sc}\sin i_{rel})^2 + (v_{sc}\cos\gamma_{sc}\cos i_{rel})^2\\ &\quad = (v_{sc}\cos\gamma_{sc})^2 = (h_{sc}/r_{enc})^2 = \mu_{cb}p_{sc}/(r_{enc}^2)\\ &\quad \Rightarrow \mu_{cb}p_{sc}/(r_{enc}^2) = [v_\infty(\cos\alpha\cos\gamma_{ga} - \sin\alpha\cos\kappa\sin\gamma_{ga})\\ &\quad + v_{ga}\cos\gamma_{ga}]^2 + (v_\infty\sin\alpha\sin\kappa)^2\end{aligned} \tag{28}$$

Once the encounter distance and the v-infinity magnitude (and the other GA body's parameters) are known, Eqs. (26) and (28) and can be used to find orbits satisfying the constraint on the ring-plane crossing distance [Eq. (27)].

Effects of Solar Gravity by Quadrant

Even at Saturn, which lies a distance of 9–10 astronomical units from the sun, the impact of the sun as a perturbing force can be significant on large orbits. The direction of the perturbing tidal acceleration that originates with solar gravity depends on the orientation of the spacecraft's orbit relative to the sun and Saturn (see Patterson et al. [4], Davis et al. [5], Yamakawa et al. [42], Howell et al. [43], and Villac and Scheeres [44]). Thus, to investigate this force and exploit it for trajectory design, observation from the perspective of a coordinate frame that rotates with Saturn about the sun is insightful. A Saturn-centered rotating frame is defined to facilitate the analysis, because the tidal field is stationary in the rotating frame. Let the $\hat{x}$-$\hat{y}$ plane represent Saturn's orbital plane. The $\hat{x}$ axis is fixed along the sun–Saturn line, and the $\hat{y}$ axis is perpendicular to the $\hat{x}$ axis in Saturn's orbital plane. The $\hat{y}$ axis is defined as positive in the direction of Saturn's motion. Four quadrants, centered at Saturn, are defined in the rotating frame and appear in Fig. 3. The quadrants are defined in a counterclockwise fashion, with quadrant I on the antisun side of Saturn and leading Saturn in its orbit. When one revolution of the spacecraft orbit is viewed in this rotating frame, its orientation is defined by the quadrant that contains the orbit apoapsis. In the current work, the angle of orientation ϕ is defined as the angle from the sun–Saturn line. The positive sense of the angle is defined in Fig. 3. The direction of the tidal acceleration in each quadrant appears in Davis et al. [5].

Consider a prograde orbit large enough to be perturbed significantly by the sun but sufficiently small such that the solar gravitational perturbations do not cause the orbit to become retrograde or to escape. Whereas the net effects on the orbital elements over multiple revolutions average to zero as the orbit precesses through the quadrants, the effects on a single revolution can be significant and may be exploited to accomplish specific mission goals. From one periapsis passage to the next, if the apoapsis originally lies in quadrants I or III, solar gravity will lower the periapse radius, increase eccentricity, and increase v_∞ with respect to Titan at a subsequent encounter. Alternatively, if apoapsis lies in quadrants II or IV, solar gravity will raise the periapse radius, decrease eccentricity, and decrease v_∞ with respect to Titan. These results are summarized in Table 1. For further discussion of changes in orbital elements due to tidal acceleration, see Davis et al. [5].

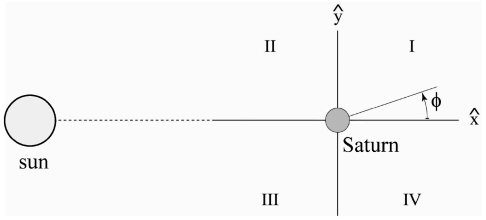

Fig. 3 Quadrants and orientation angle as defined in the rotating frame (Davis et al. [5]).

For a given orbit at a specified orientation angle, the solar gravitational perturbations have maximum effect when the orbit lies in the ecliptic plane. It is noted that Saturn's equatorial plane is inclined at about 26.7 deg with respect to the ecliptic. Also, within each quadrant, solar perturbations are at a maximum when the apoapsis lies at approximately 45 deg from the sun–Saturn line (see Fig. 3), although the precise value of the quadrant angle corresponding to the maximum can vary significantly as the period of the orbit changes. Especially for large orbits, the orientation of the sun–Saturn line with respect to the spacecraft orbit line of apsides shifts due to Saturn's motion about the sun while the spacecraft is in transit about Saturn, affecting the value of the optimal orientation. The changes in semimajor axis, periapse radius, and eccentricity from one revolution to the next as functions of quadrant angle ϕ for a 957-day orbit appear in Fig. 4. Of course, once $\phi > 90$ deg, the orbit has shifted from quadrant I to quadrant II. Thus, the quantities increase and decrease consistent with the quadrant.

The solar effects on an orbit increase as the apoapse radius increases. Thus, for long-period orbits, the effects of solar gravity can be significant. For an orbit of sufficiently large period, with apoapsis in quadrant I or quadrant III, solar gravity can lower periapse radius such that impact with the planet occurs.

Numerical Results

Assumptions and Constraints

The Cassini primary mission was completed in July 2008 with an extended mission expected to last until June 2010. Table 2 summarizes the initial condition for the end-of-mission scenarios that originates from the end of the proposed extended mission [12]. The assumption is made that a trajectory ends in impact when the periapse radius r_p is less than one Saturnian radius, 1 R_S.

The end-of-mission options are subjected to the following general constraints:

1) The ΔV budget is 50 m/s;

2) The minimum flyby altitude at Titan is 1000 km (the last Titan flyby is allowed to be 900 km);

Table 1 Effects of solar gravitational perturbations relative to the previous orbit, measured from periapsis to periapsis (Davis et al. [5])

Parameter	Apoapsis located in quadrants I and III	Apoapsis located in quadrants II and IV
Semimajor axis	Decreases	Increases
Periapsis radius	Decreases	Increases
Eccentricity	Increases	Decreases
v_∞ relative to Titan	Increases	Decreases

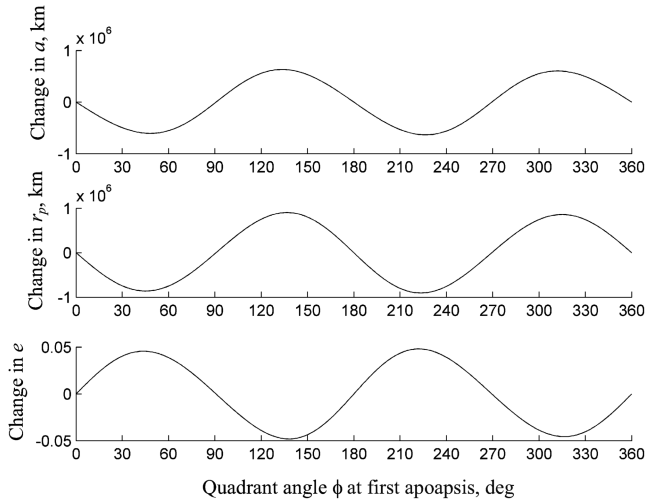

Fig. 4 Changes in orbital elements from one revolution to the next as a function of quadrant angle ϕ: 957-day orbit (Davis et al. [5]).

3) The spacecraft should not cross the rings of Saturn [see Eq. (27)] to avoid damaging the spacecraft (except when it is during its final ring-plane crossing before impacting Saturn);

4) The time for a cleanup maneuver after the last Titan flyby should be minimized.

Models for Trajectory Design and Trajectory Propagation

Patched-Conic Propagation

A patched-conic propagator called the satellite tour design program (STOUR) is used to calculate short-period impact trajectories. STOUR is a software tool developed by the Jet Propulsion Laboratory (JPL) for the Galileo mission design [45]. The program has been enhanced and extended at Purdue University to perform automated design of gravity-assist tours of the solar system and of the satellite system of Jupiter [46–49]. STOUR uses the patched-conic method to calculate gravity-assist trajectories meeting specified requirements. Results obtained from STOUR can be used as a starting guess for numerical integration and optimization in a higher-fidelity model. Table 3 shows the parameters of Saturn and Titan used by STOUR in the short-period impact analysis.

Model for Long-Period Orbits

Long-period orbits are numerically computed with a Runge–Kutta 4(5) integrator. Initial conditions and gravitational parameter values for the sun and Saturn are extracted from the JPL DE408 ephemeris[††] and for Titan from the SAT424L ephemeris. Their positions are then integrated along with the spacecraft state. All integrations are performed in the Earth equator and equinox of J2000 inertial frame. The integration software was verified by the full ephemeris, multibody package Generator-C, developed at Purdue [50]. The constants and assumptions used in this analysis are listed in Table 4.

Summary of Impact Trajectories

Two Saturn impact options are presented for Cassini end-of-mission: a short-period option and a long-period option. For the short-period impact, the spacecraft lowers its periapsis by successive Titan-to-Titan resonant transfers. The spacecraft enters the F–G ring gap with a period of 6–10 days and an inclination of 50–70 deg and encounters Titan again to reduce the periapsis below Saturn's atmosphere. Depending on Titan's location at encounter (i.e., the radial distance from Saturn), a list of resonant orbits (e.g., 1:2, 3:5, 4:9) are possible to achieve an impact and also to satisfy the constraint on the node distance (as presented in Table 5). It is noted that the maneuver costs for short-period trajectories are zero in the patched-conic model. In a higher-fidelity model that includes J_2 perturbations, however, a nonzero maneuver cost is expected: the J_2 perturbation can rotate the line of apsides and the line of nodes and thus a maneuver may be required to correct the trajectory for the next targeted Titan flyby. (For detailed descriptions on how J_2 perturbations affect orbits about Saturn, see Buffington and Strange [51].)

For long-period orbits with periods of 850–1116 days and longer, Saturn impact can be achieved using solar perturbations together with an apoapse ΔV (from 0 to 50 m/s) to lower the periapsis into Saturn's atmosphere. The orientation of the spacecraft orbit must remain near 45 deg in quadrants I and III (see Fig. 3) relative to the sun–Saturn line and the inclination can range from 0 to 40 deg. The desired orientation can be reached via a series of alternating outbound–inbound and inbound–outbound transfers (see Wolf and Smith [10] for detailed descriptions). Assuming the spacecraft is in a 16-day orbit (as shown in Table 2), the total time required (before the final Titan flyby) is ~290 days, which requires seven Titan flybys. For periods >1100 days, the solar perturbation alone can be sufficient (i.e., no apoapse maneuver is necessary) to reduce the periapsis down to below 1 R_S, providing an attractive flyby-and-forget option (i.e., the spacecraft will impact Saturn without any control once the final Titan flyby is performed correctly) for a Cassini end-of-mission scenario.

Option 1: Saturn Impact via Short-Period Orbit

To find short-period impact trajectories, orbits at Saturn with a constant v_∞ relative to Titan are first characterized. According to the Tisserand criterion in Eq. (14), for any given two of a_{sc}, p_{sc}, and i_{rel}, the remaining one of the three orbital parameters can be calculated. The semimajor axis a_{sc} is related to the orbital period T_{sc} from Eq. (2), and the semilatus rectum p_{sc} is related to the vacant node distance r_{vac} from Eq. (26).

Figure 5 is a Tisserand graph that shows a sampling of the $T_{sc} - r_{vac} - i_{rel}$ (i.e., orbital period, vacant node crossing distance, and inclination relative to Titan's orbit) solution space for a v_∞ of 5.490 km/s (taken from Table 2), where the third dimension of i_{rel} is indicated by contour lines. The shaded areas (in gray) are regions of the rings through which the spacecraft is not allowed to pass [i.e., the constraint on the node distance given by Eq. (27)]. Impact trajectories with a vacant node distance of one Saturnian radius (for $i_{rel} = 30$ and 60 deg) are indicated with asterisks. (To simplify the calculations here, $r_{vac} = 1\ R_S$ is used instead of $r_p = 1\ R_S$.) In terms of the sequence of Titan-to-Titan transfers, impact orbits correspond to the ultimate (i.e., final) Titan flyby. To find penultimate (i.e., second-to-last) orbits, consider a reverse of the ultimate Titan flyby: the incoming excess velocity vector $\mathbf{V}_{\infty,\mathbf{in}}$ is derived from an impact orbit (i.e., an asterisk) and the family of the outgoing orbits is determined by setting the flyby altitude to its minimum (i.e., 900 km) with a sampling of the B-plane angle from −180 to 180 deg. The two ovals in Fig. 5 are families of penultimate orbits that impact Saturn with inclinations of 30 and 60 deg. (Ovals with other inclination values can also be plotted in Fig. 5 but for the purpose of clear illustration, only two ovals are depicted.) The ovals demarcate the

Table 2 Initial condition for Cassini end-of-mission scenario

Parameter	Values
Titan encounter time	21 June 2010, 1:28:22
Titan's distance from Saturn	20.21 R_S
v_∞ with respect to Titan[a]	5.490 km/s
Pump angle[a]	119.4 deg
Crank angle[a]	1.107 deg
Orbital period[a]	15.9 days
Periapse radius[a]	2.63 R_S
Inclination (wrt Saturn's equator)[a]	1.71 deg
Apoapse orientation (wrt the sun)[a]	$\phi = 270.6$ deg

[a]Preencounter conditions.

[††]Data available online at ftp://naif.jpl.nasa.gov/pub/naif/generic_kernels/spk/planets/a_old_versions/de408.bsp [cited 15 Dec. 2008].

Table 3 Constants for patched-conic analysis

Parameter	Values
Gravitational parameter of Saturn, $\mu_{\text{Saturn}} = \mu_{\text{cb}}$	3.79312692×10^7 km^3/s^2
Radius of Saturn, R_S	60,268 km
Gravitational parameter of Titan, $\mu_{\text{Titan}} = \mu_{\text{ga}}$	8978.2 km^3/s^2
Radius of Titan, R_T	2575 km
Orbital period of Titan, $T_{\text{Titan}} = T_{\text{ga}}$	15.945 days
Semimajor axis of Titan's orbit, $a_{\text{Titan}} = a_{\text{ga}}$	1.221215×10^6 km (=20.263 R_S)
Eccentricity of Titan's orbit, $e_{\text{Titan}} = e_{\text{ga}}$	0.0288
Inclination[a] of Titan's orbit, $i_{\text{Titan}} = i_{\text{ga}}$	0.365 deg

[a]Inclination relative to Saturn's equator.

Table 4 Constants and assumptions for numerical integrations

Parameter	Values
μ_{Saturn}	$3.794062606113728 \times 10^7$ km^3/s^2
μ_{sun}	$1.327124400179870 \times 10^{11}$ km^3/s^2
μ_{Titan}	$8.978137176189042 \times 10^3$ km^3/s^2
Julian date of epoch	2,455,660.40139
Reference frame	Earth's equator and equinox of J2000
Integrator	Runge–Kutta 4(5)
Tolerances, relative and absolute	10^{-12}
Ephemeris for Saturn	DE408
Ephemeris for Titan	SAT424L

boundaries within which orbits fly by at altitudes higher than 900 km (i.e., satisfy the altitude constraint at Titan). These ovals are essentially projections of the $\mathbf{V}_{\infty,\mathbf{out}}$ circles illustrated in Fig. 1 (which are determined by the maximum bending angle δ) mapped over the $T_{\text{sc}} - r_{\text{vac}} - i_{\text{rel}}$ solution space.

Among the two ovals of penultimate orbits in Fig. 5, only one of them (the impact with an inclination of 60 deg) extends to the gap between the F and G rings (i.e., a feasible region). The crosshatched region in Fig. 5 contains the set of periods T_{sc} and inclinations i_{rel} required for feasible penultimate orbits (which can impact Saturn after a single Titan flyby). Note that the set of candidate penultimate orbits consists of highly inclined orbits, each with $i_{\text{rel}} > 50$ deg. The reason for the high inclination is that, for a given orbital period, as inclination increases, the absolute value of the flight-path angle decreases toward zero. Hence, for a short-period orbit ($T_{\text{sc}} < T_{\text{ga}}$), the gravity assist occurs closer and closer to apoapsis with increasing inclination. A flyby at Titan (with the same altitude) is therefore more effective for orbits with high inclination when the encounter is near apoapsis. The maximum inclination of Cassini's orbit is ~75 deg for $v_\infty = 5.490$ km/s (an expression of maximum inclination can be found in Uphoff et al. [13]).

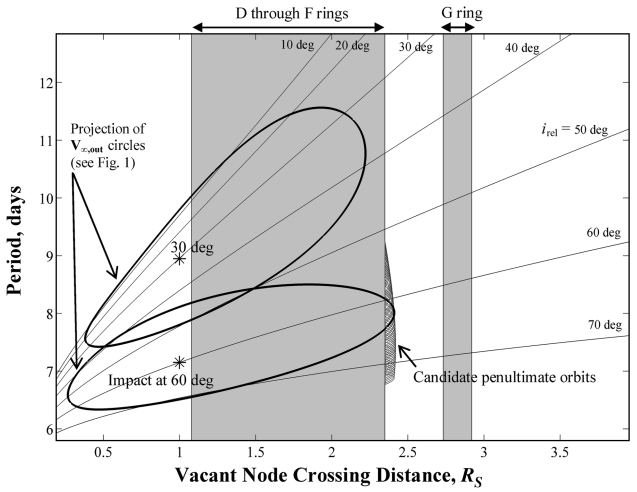

Fig. 5 Tisserand graph for the design of gravity-assist trajectories that impact Saturn ($v_\infty = 5.490$ km/s, $h_p = 900$ km, $r_{\text{enc}} = 20.21\ R_S$, $\gamma_{\text{sc}}\gamma_{\text{ga}} > 0$).

All "pockets" of candidate penultimate orbits in Fig. 5 are collected and plotted in Fig. 6 (indicated by the second curve from the right). Also plotted in Fig. 6 are penultimate orbits with different encounter conditions at Titan (i.e., the radial distance of Titan from Saturn at encounter r_{enc} and the sign of the product of the flight-path angles $\gamma_{\text{sc}}\gamma_{\text{ga}}$). Note that the range of periods and inclinations of penultimate orbits widens as the Titan encounter distance r_{enc} increases. An intuitive explanation is that the encounter distance r_{enc} acts as a leveraging arm of an apoapse ΔV to reduce the periapsis of the spacecraft orbit (where a Titan flyby can be thought as an equivalent velocity change relative to Saturn); the longer the encounter distance, the more effective the ΔV in reducing the periapsis ($<1\ R_S$).

Some orbits from Fig. 6 are selected (based on whether the period makes a rational fraction with Titan's orbital period) and their characteristics summarized in Table 5. The pump and crank angles provided in Table 5 are for the convenience of using a patched-conic propagator like STOUR. (STOUR asks the user to input the resonance ratio and the change in crank angle for each event.) Table 5 provides a range of selection of impact trajectories (for different Titan encounter conditions) that can impact Saturn in 4–9 months (112–287 days) using 5–10 Titan flybys. Periods of the penultimate orbits range from 6 to 10 days with inclinations of ~50 to 70 deg. To achieve an impact from a 16-day equatorial orbit, mission designers should first crank up the inclination to 40–50 deg (in 1:1 resonant orbits), then pump down the period (and crank up the inclination together) using 3:4 and 3:5 resonant orbits. The higher the inclination and the lower the period of the penultimate orbits, the more intermediate Titan flybys are required (in general) to achieve an impact.

Choice of Sampling Parameter

As a side note, some details of sampling the orbital parameters for creating Fig. 5 are described. Using the Tisserand criterion in Eq. (14) requires a sampling of a_{sc}, p_{sc}, and i_{rel}, which represents a search space of three parameters with one constraint. An alternative

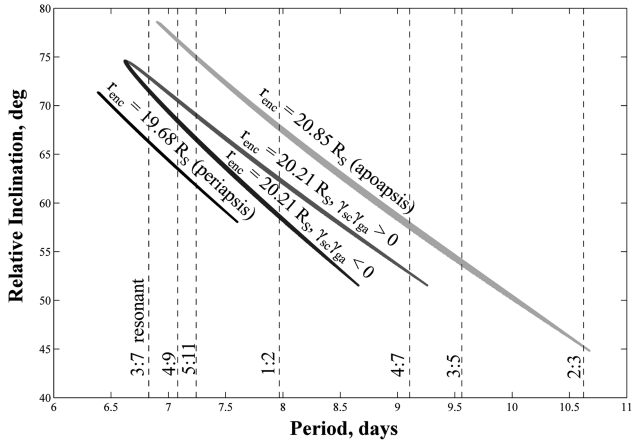

Fig. 6 Penultimate impact orbits with node crossing inside the ring gap ($v_\infty = 5.490$ km/s, $h_p = 900$ km).

Table 5 Selected penultimate impact trajectories

Titan: sc revs	Period, days	Inclination, deg[a]	Pump angle, deg	Crank angle, deg[b]	Number of Titan flybys[c]	Min flyby altitude, km[d]	Total TOF, days[e]
			$v_\infty = 5.490$ km/s, $r_{enc} = 20.21\ R_S$, $\gamma_{sc}\gamma_{ga} > 0$				
1:2	7.97	62.30	142.0	42.06	7	1000	159
3:7	6.83	72.85	151.1	66.72	10	1000	287
4:7	9.11	52.75	136.0	32.17	6	900	191
4:9	7.09	70.45	148.6	57.52	9	1000	239
			$v_\infty = 5.490$ km/s, $r_{enc} = 20.21\ R_S$, $\gamma_{sc}\gamma_{ga} < 0$				
1:2	7.97	58.45	142.0	40.03	7	1000	159
3:7	6.83	71.40	151.1	65.66	10	1000	287
4:9	7.09	68.30	148.6	56.25	8	1000	223
			$v_\infty = 5.490$ km/s, $r_{enc} = 20.85\ R_S$ (apoapsis)				
1:2	7.97	67.50	144.4	45.86	8	1000	175
2:3	10.63	45.19	132.0	25.47	5	900	112
3:5	9.57	53.60	135.9	31.48	5	1000	128
4:7	9.11	57.30	138.0	34.51	6	1000	223
4:9	7.09	76.55	151.8	68.47	10	1000	255
			$v_\infty = 5.490$ km/s, $r_{enc} = 19.68\ R_S$ (periapsis)				
3:7	6.83	66.20	148.5	56.52	9	900	223
4:9	7.09	63.40	146.3	50.03	8	900	223
5:11	7.25	61.71	145.0	46.97	8	900	239

[a]Relative to Titan's orbit plane.
[b]Only the principal values of the crank angle κ are presented. Other quadrants of κ can be calculated from the principal values.
[c]Number of Titan flybys required to impact Saturn from a 16-day equatorial orbit.
[d]Minimum flyby altitude of the final Titan flyby (all nonultimate flybys have altitudes $\geq$ 1000 km).
[e]Total flight time from a 16-day equatorial orbit to final Titan flyby (exclude time to impact).

approach described in Strange et al. [33] uses two angles (e.g., the pump and crank angles) as sampling parameters, which results in a search space of two parameters with no constraint. Both approaches can be applied to the design of gravity-assist trajectories in many applications. In this work, the former approach is employed as it allows a direct search of orbital parameters within the region of interest (i.e., short-period trajectories that satisfy the constraints on r_{vac}). On the other hand, the latter approach can be more convenient for a global search on a broad range of design space [52].

Short-Period Impact Trajectory

As an example, a short-period impact trajectory propagated using a high-fidelity mission design program called Computer Algorithm for Trajectory Optimization [53] (CATO) is presented. CATO is a multimission optimization program that numerically integrates the equations of motion of a point-mass spacecraft subject to gravitational accelerations due to any combination of sun, planets, and satellites of the central body, including their oblateness. For a given sequence of gravity assists, an optimal solution is found by minimizing the total deterministic ΔV. A sample impact trajectory is detailed and illustrated in Table 6 and Fig. 7, respectively. The trajectory is first built using either a patched-conic method (STOUR), or a "patched-integrated" method (which includes J_2) [51], and then integrated and optimized by CATO.

The initial state of the impact trajectory is taken from Table 2 (i.e., end of the proposed extended mission). The inclination of the spacecraft orbit is first cranked up to ~40 deg with three 1:1 resonant transfers. Then the period is pumped down (and the inclination is cranked up simultaneously) with a 3:4 and a 3:5 resonant orbit. Next, a 1:2 resonant orbit (8-day period) is used to place the vacant node at the inner edge of the F–G gap at a 62.5 deg inclination. As previously shown in Fig. 6, impact trajectories can be achieved from inclinations >45 deg. However, a 62.5 deg inclination (near the critical inclination) is chosen to minimize ΔV costs associated with correcting J_2 perturbations necessary to

Table 6 Short-period Saturn impact trajectory

Event	Titan: sc	Encounter date yyyy/mm/dd	In/ out	h_p, km	θ, deg	v_∞, km/s	Period, day[a]	r_p, R_S[b]	Inc., deg[c]	r_{vac}, R_S[d]	TOF, day[e]
1	1:1	2010/06/21	Out	1000	−92.6	5.49	15.9	3.00	18.4	3.16	15.9
Maneuver		2010/06/30					$\Delta V = 9.74$ m/s				
2	1:1	2010/07/07	Out	1000	−99.0	5.49	15.9	3.83	32.5	4.19	15.9
Maneuver		2010/07/15					$\Delta V = 6.25$ m/s				
3	1:1	2010/07/22	Out	1000	−104	5.49	15.9	5.23	42.2	5.86	15.9
Maneuver		2010/07/31					$\Delta V = 0.49$ m/s				
4	3:4	2010/08/07	Out	1000	−166	5.48	11.9	4.47	50.4	4.78	47.8
Maneuver		2010/08/29					$\Delta V = 6.05$ m/s				
5	3:5	2010/09/24	Out	1000	−176	5.49	9.59	3.73	58.0	3.87	47.8
Maneuver		2010/09/27					$\Delta V = 0.95$ m/s				
Maneuver		2010/10/20					$\Delta V = 0.53$ m/s				
6	1:2	2010/11/11	Out	1440	145	5.49	8.15	2.37	62.5	2.40	15.9
Maneuver		2010/11/17					$\Delta V = 3.62$ m/s				
7	N/A	2010/11/27	Out	900	99.5	5.49	7.16	1.00	59.6	1.01	5.1[f]
Total maneuver cost							$\Delta V = 27.6$ m/s				

[a]Postflyby orbital period.
[b]Postflyby periapsis radius.
[c]Postflyby inclination relative to Saturn's equator.
[d]Postflyby vacant node crossing distance.
[e]Time of flight to the next Titan encounter.
[f]Impact occurs 5.1 days after the final Titan flyby.

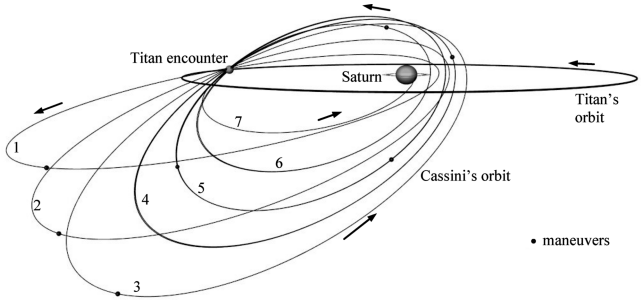

Fig. 7 Saturn impact trajectory via ring gap hopping.

reencounter and target the final Titan flyby. A final Titan flyby then lowers the periapsis to 1.00 R_S (60,330 km) and the spacecraft impacts Saturn's atmosphere 5 days later. The total time to impact (from the initial condition of Table 2) is 160 days; seven Titan flybys are required for this scenario. It is noted that the results found by patched-conic analysis from Table 5 (on the 1:2 case for $r_{\text{enc}} = 20.21\ R_S$, $\gamma_{\text{sc}}\gamma_{\text{ga}} > 0$) match closely with the numerically integrated trajectory in Table 6 in terms of period and inclination of the penultimate orbit, number of Titan flybys, and the total time of flight (TOF). However, for the final Titan flyby, patched-conic analysis predicts that an altitude of 1000 km is sufficient to impact Saturn, whereas the numerically integrated trajectory requires an altitude of 900 km. Also, the patched-conic solution does not require any ΔV for the Titan-to-Titan transfer, but the numerically integrated solution requires a total deterministic ΔV of 27.6 m/s to maintain the targeted Titan flybys (mainly due to J_2 perturbations).

Option 2: Saturn Impact via Long-Period Orbit

To achieve impact in the long-period strategy, solar gravity is used to lower the periapses of orbits whose apoapses lie in quadrant III. With a sufficiently large orbit oriented and inclined favorably, the spacecraft can impact Saturn with low ΔV or without a maneuver at apoapsis.

Table 7 ΔV at apoapsis and subsequent periapse radii

Period	ΔV, m/s	Postmaneuver r_p, R_S
877 days	0	3.02
877 days	47	0.97
957 days	0	1.82
957 days	21	0.99
1116 days	0	0.20

Final Titan Flyby

Analysis for a long-period impact originates with initial conditions from STOUR for an outbound Titan flyby on 8 April 2011, after a series of seven flybys (from the initial condition of Table 2) that serve to pump up and reorient the orbit. The penultimate orbit is assumed to be in a 5:1 resonance with Titan, which is associated with a period of 80 days. It is inclined at 25.8 deg with respect to (wrt) Saturn's equator, corresponding to a 0.9 deg inclination with respect to Saturn's ecliptic plane. The periapse radius before the Titan flyby is 5.58×10^5 km, or 9.26 R_S.

The flyby conditions (i.e., flyby altitude and B-plane angle) are adjusted to yield postflyby orbits of different periods, ranging from 877 to 1116 days. The inclination of these postflyby trajectories relative to Saturn's ecliptic plane is approximately 2 deg. Each of the orbits lies in quadrant III. The quadrant angles range from $\phi = 217$ deg for the largest orbit to $\phi = 222$ deg for the smallest orbit. If solar gravity is not modeled, the periapse radius of each of the postflyby orbits is approximately 7.23×10^5 km, or 12 R_S. However, solar gravity significantly affects the orbits, resulting in naturally reduced periapse radii. The investigation focuses on the effect of solar perturbations on orbits with periods of 877, 957, and 1116 days. Table 7 summarizes the subsequent periapse radii and the ΔV required for Saturn impact.

Results

The two largest postflyby orbits are characterized by periods of 957 and 1116 days. After departing the region of Titan, the trajectories reach apoapse radii of 3.66×10^7 km (608 R_S) and 4.09×10^7 km (679 R_S), respectively. Although no ΔV is applied, solar gravity slows the spacecraft and decreases the periapse radius of each orbit. The periapse radius of the 1116-day orbit is lowered to 1.18×10^4 km (0.20 R_S), and the spacecraft impacts Saturn without a maneuver. The subsequent periapse radius of the 957-day orbit, on the other hand, is 1.09×10^5 km (1.82 R_S), still above the surface of Saturn. A maneuver may be implemented at apoapsis to further lower the periapsis and achieve impact. With a ΔV of 21 m/s applied at apoapsis, the periapse radius of the 957-day orbit becomes 5.99×10^4 km (0.99 R_S), and the spacecraft impacts Saturn. Similarly, with a ΔV of 47 m/s applied at apoapsis, a spacecraft following the 877-day trajectory impacts Saturn. Although specific trajectory characteristics will change with different postflyby conditions, these particular examples may serve as a guide in relating orbit size and apoapse ΔV requirements for Saturn impact. Titan encounters can be used to deliver the spacecraft to orbits of different periods and orientations as desired. Minor adjustments to orientation and inclination (via the final Titan encounter) can change the impact conditions.

Table 8 Long-period Saturn impact trajectory

Event	Titan: s/c	Encounter date yyyy/mm/dd	In/out	h_p, km	θ, deg	v_∞, km/s	Period, day[a]	r_p, R_S[b]	Inc., deg[c]	TOF, day[d]
1	1:1	2010/06/21	Out	1000	−92.6	5.49	15.9	3.00	18.4	15.9
Maneuver		2010/06/30					$\Delta V = 5.48$ m/s			
2	3:2	2010/07/07	Out	1000	28.0	5.49	23.8	4.19	8.73	47.8
Maneuver		2010/07/21					$\Delta V = 6.16$ m/s			
3	4:2[e]	2010/08/23	OI[e]	1349	46.0	5.49	36.2	5.41	0.44	68.6
4	2:1	2010/10/31	In	1658	−77.3	5.50	31.9	5.22	11.1	31.9
5	3:1	2010/12/02	In	1000	−119	5.49	47.8	7.04	19.5	47.8
Maneuver		2010/12/20					$\Delta V = 1.22$ m/s			
6	5:1	2011/01/19	In	1000	−115	5.49	79.8	9.26	25.8	79.7
Maneuver		2011/02/16					$\Delta V = 1.76$ m/s			
7	70:1	2011/04/08	In	1000	−162	5.48	1116	0.22	25.1	1119[f]
Total maneuver cost							$\Delta V = 14.62$ m/s			

[a]Postflyby orbital period.
[b]Postflyby periapsis radius.
[c]Postflyby inclination relative to Saturn's equator.
[d]Time of flight to the next Titan encounter.
[e]Nonresonance transfer (outbound to inbound).
[f]Impact occurs 1119 days after the final Titan flyby.

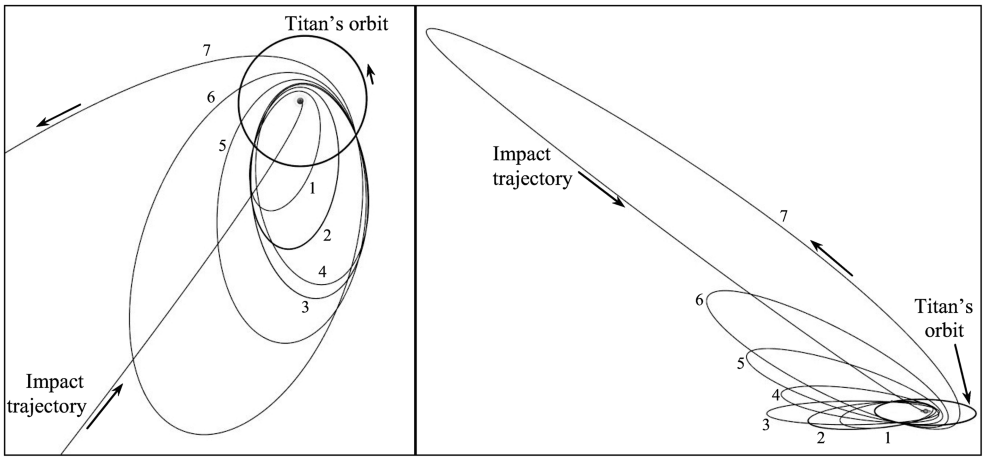

Fig. 8 Long-period impact trajectory, plotted in a Saturn-centered inertial frame.

Orientation and Inclination Requirements

The orbital period required for impact depends on the inclination and orientation of the orbit as well as the epoch and initial periapse radius of the orbit. For example, if the initial periapse radius of the postflyby orbit (immediately after the final Titan flyby) is smaller, a trajectory with a shorter period can lead to impact. The optimal orientation in quadrant III, which depends on an orbit's size, inclination, and other characteristics, is approximately 219 deg for the aforementioned 1116-day orbit. The orientation of this trajectory must be within 20 deg of the optimal orientation to achieve impact without an applied ΔV. If the inclination of the orbit is higher or if the initial periapse radius is larger, the orientation window will decrease in size. The optimal inclination of the orbit is 0 deg relative to the ecliptic plane. For the 1116-day trajectory, impact has been confirmed for inclinations up to about 40 deg relative to the ecliptic plane. For smaller trajectories or those further from the optimal orientation angle, this upper limit on inclination will decrease.

End-to-End Example

The usefulness of this technique is demonstrated by the development of a long-period impact trajectory in a higher-fidelity model. Starting from the initial condition in Table 2, a patched-conic solution found by STOUR is taken as a first guess for CATO [53]. Table 8 shows an end-to-end impact trajectory integrated in a full ephemeris model using CATO; the trajectory appears in Fig. 8. A total deterministic ΔV of 14.62 m/s is used to target the desired sequence of Titan flybys. First, the inclination of the orbit is dropped into Saturn's equatorial plane, visible in orbits 1–2 in Fig. 8, and a 36-day orbit, orbit 3 in Fig. 8, reorients the spacecraft apoapsis such that $\phi \sim 220$ deg. Four more Titan flybys in resonant transfers follow, pumping up the orbital period from 32 to 1116 days and raising the inclination into Saturn's orbital plane, depicted in orbits 4–7 in Fig. 8. After the final Titan flyby, with no additional ΔV required, solar gravity decreases periapse radius to 0.22 R_S, and the spacecraft impacts Saturn on 2 May 2014. The total time of flight from the initial conditions to Saturn impact is 1411 days, with a total of seven Titan flybys.

Conclusions

Several end-of-mission scenarios are being considered for the Cassini mission, including injection into a 500-year stable orbit within the Saturnian system, escape from Saturn to impact on a gas giant, and impact in the Saturnian atmosphere itself. The orbit design is constrained by available propellant and spacecraft lifetime. In this investigation, two strategies are presented for achieving Saturn impact for the Cassini spacecraft with a low ΔV budget. The first involves a short-period final orbit with a period of 6–10 days. In this short-period case, a new application of the Tisserand graph is successfully employed to avoid collision with the rings during multiple ring-plane crossings while guaranteeing atmospheric entry. A sample trajectory impacts Saturn after 159 days of flight, involving six Titan encounters with a total deterministic ΔV of 27.6 m/s. The long-period case employs solar gravity to naturally reduce spacecraft periapsis. This approach involves a large final orbit oriented with respect to the sun so that the gravitational perturbations, significant in this regime, slow the spacecraft and lead to impact with or without a small ΔV at apoapsis. In particular, a final orbit is determined in which solar perturbations automatically lower the periapsis into Saturn's atmosphere. The final Titan flyby, if performed accurately enough, therefore provides a flyby-and-forget option: after the last flyby of Titan is performed, the spacecraft is guaranteed to impact Saturn without further action from the spacecraft or the Cassini operations team. A sample trajectory demonstrating the success of this strategy involves a final orbit with a Keplerian period of 1116 days. Although the whole process from the end of the extended mission to impact takes 1411 days, the final Titan flyby takes place after 327 days of pumping up and orienting the orbit. The spacecraft makes six Titan encounters and uses a total ΔV of 14.6 m/s before the final Titan flyby.

These two design strategies have been successfully employed to develop potential Saturn impact orbits for the Cassini end-of-mission scenario. However, both are applicable to other missions. The use of the Tisserand graph may assist in the design of future Saturn tours to safely navigate the ring gap, as well as potentially to design tours of moons at Jupiter or Saturn. The effect of solar gravity on a large orbit can be employed not only to decrease the periapse radius as demonstrated in this investigation, but by adjusting the orientation of the orbit, also to raise periapsis and decrease the eccentricity of a large orbit for other trajectory design applications.

Acknowledgments

This work has been supported in part by the Jet Propulsion Laboratory, California Institute of Technology, under Contract Number 1283234 (Jeremy B. Jones, Technical Manager) with NASA. We are grateful to Jeremy B. Jones and Nathan J. Strange for providing useful information, guidance, and helpful suggestions. We thank Todd Brown and Chris Patterson for their assistance with the trajectory plotting. We also thank Kevin W. Kloster for his contributions in maintaining and updating the satellite tour design program at Purdue. Portions of this work were also supported by Purdue University.

References

[1] Mitchell, R. T., "Cassini/Huygens at Saturn and Titan," International Astronautical Congress Paper 05-A3.2.A.01, Oct. 2005.

[2] *Planetary Protection Provisions for Robotic Extraterrestrial Missions*, NASA NPR 8020.12C, April 2005.

[3] Bindschadler, D. L., Theilig, E. E., Schimmels, K. A., and Vandermey, N., "Project Galileo: Final Mission Status," International Astronautical Congress Paper 03-Q.2.01, Sept.–Oct. 2003.

[4] Patterson, C., Kakoi, M., Howell, K. C., Yam, C. H., and Longuski, J. M., "500-Year Eccentric Orbits for the Cassini Spacecraft Within the Saturn System," American Astronautical Society Paper 07-256, Aug. 2007.
[5] Davis, D. C., Patterson, C., and Howell, K. C., "Solar Gravity Perturbations to Facilitate Long-Term Orbits: Application to Cassini," American Astronautical Society Paper 07-275, Aug. 2007.
[6] Okutsu, M., Yam, C. H., Longuski, J. M., and Strange, N. J., "Cassini End-of-Life Escape Trajectories to the Outer Planets," American Astronautical Society Paper 07-258, Aug. 2007.
[7] Strange, N. J., Goodson, T. D., and Hahn, Y., "Cassini Tour Redesign for the Huygens Mission," AIAA Paper 2002-4720, Aug. 2002.
[8] Smith, J. C., "Description of Three Candidate Cassini Satellite Tours," American Astronautical Society Paper 98-106, Feb. 1998.
[9] Wolf, A. A., "Touring the Saturnian System," *Space Science Reviews*, Vol. 104, Nos. 1–4, July 2002, pp. l01–128. doi:10.1023/A:1023692724823
[10] Wolf, A. A., and Smith, J. C., "Design of the Cassini Tour Trajectory in the Saturnian System," *Control Engineering Practice*, Vol. 3, No. 11, Oct. 1995, pp. 1611–1619. doi:10.1016/0967-0661(95)00172-Q
[11] Goodson, T. D., Ballard, C. G., Gist, E. M., Hahn, Y., Stumpf, P. W., Wagner, S. V., and Williams, P. N., "Cassini–Huygens Maneuver Experience: Ending the Prime Mission," AIAA Paper 2008-6751, Aug. 2008.
[12] Buffington, B., Strange, N., and Smith, J., "Overview of the Cassini Extended Mission Trajectory," AIAA Paper 2008-6752, Aug. 2008.
[13] Uphoff, C., Roberts, P. H., and Friedman, L. D., "Orbit Design Concepts for Jupiter Orbiter Missions," *Journal of Spacecraft and Rockets*, Vol. 13, No. 6, 1976, pp. 348–355. doi:10.2514/3.57096
[14] Vandermey, N., and Paczkowski, B. G., "The Cassini–Huygens Mission Overview," AIAA Paper 2006-5502, June 2006.
[15] "Cassini Saturn Orbiter and Titan Probe, ESA/NASA Assessment Study," ESA SCI(85)1, Aug. 1985.
[16] Spilker, L. J. (ed.), *Passage to a Ringed World*, NASA Special Publ., NASA SP-533, Oct. 1997.
[17] Miner, E. D., "The Cassini–Huygens Mission to Saturn and Titan," *ASP Conference Proceedings*, Vol. 281, Astronomical Society of the Pacific, San Francisco, 2002, pp. 373–381.
[18] Matson, D. L., Spilker, L. J., and Lebreton, J.-P., "The Cassini/Huygens Mission to the Saturnian System," *Space Science Reviews*, Vol. 104, Nos. 1–4, July 2002, pp. 1–58. doi:10.1023/A:1023609211620
[19] Cuzzi, J. N., Colwell, J. E., Esposito, L. W., Porco, C. C., Murray, C. D., Nicholson, P. D., Spilker, L. J., Marouf, E. A., French, R. C., Rappaport, N., and Muhleman, D., "Saturn's Rings: Pre-Cassini Status and Mission Goals," *Space Science Reviews*, Vol. 104, Nos. 1–4, July 2002, pp. 209–251. doi:10.1023/A:1023653026641
[20] Porco, C. C., Helfenstein, P., Thomas, P. C., Ingersoll, A. P., Wisdom, J., West, R., et al., "Cassini Observes the Active South Pole of Enceladus," *Science*, Vol. 311, No. 5766, March 2006, pp. 1393–1401. doi:10.1126/science.1123013
[21] Hansen, C. J., Esposito, L., Stewart, A. I. F., Colwell, J., Hendrix, A., Pryor, W., Shemansky, D., and West, R., "Enceladus' Water Vapor Plume," *Science*, Vol. 311, No. 5766, March 2006, pp. 1422–1425. doi:10.1126/science.1121254
[22] Stofan, E. R., Elachi, C., Lunine, J. I., Lorenz, R. D., Stiles, B., Mitchell, K. L., et al., "The Lakes of Titan," *Nature (London)*, Vol. 445, No. 7123, Jan. 2007, pp. 61–64. doi:10.1038/nature05438
[23] Spitale, J. N., Jacobson, R. A., Porco, C. C., and Owen, W. M., Jr., "The Orbits of Saturn's Small Satellites Derived from Combined Historic and Cassini Imaging Observations," *Astronomical Journal*, Vol. 132, No. 2, Aug. 2006, pp. 692–710. doi:10.1086/505206
[24] Porco, C. C., Baker, E., Barbara, J., Beurle, K., Brahic, A., Burns, J. A., et al., "Cassini Imaging Science: Initial Results on Saturn's Rings and Small Satellites," *Science*, Vol. 307, No. 5713, Feb. 2005, pp. 1226–1236. doi:10.1126/science.1108056
[25] Flanagan, S., and F. Peralta, "Cassini 1997 VVEJGA Trajectory Launch/Arrival Space Analysis," American Astronautical Society Paper 93-684, Aug. 1993.
[26] Lebreton, J-P., Witasse, O., Sollazzo, C., Blancquaert, T., Couzin, P., Schipper, A.-M., Jones, J. B., Matson, D. L., Gurvits, L. I., Atkinson, D. H., Kazeminejad, B., and Pérez-Ayúcar, M., "An Overview of the Descent and Landing of the Huygens Probe on Titan," *Nature (London)*, Vol. 438, No. 7069, Dec. 2005, pp. 758–764. doi:10.1038/nature04347
[27] Sollazzo, C., Wheadon, J., Lebreton, J.-P., Clausen, K., Blancquaert, T., Witasse, O., Pérez-Ayúcar, M., Schipper, A.-M., Couzin, P., Salt, D., Hermes, M., and Johnsson, M., "The Huygens Probe Mission to Titan: Engineering the Operational Success," AIAA Paper 2006-5503, June 2006.
[28] Goodson, T. D., Buffington, B. B., Hahn, Y., Strange, N. J., Wagner, S. V., and Wong, M. C., "Cassini–Huygens Maneuver Experience: Cruise and Arrival at Saturn," American Astronautical Society Paper 05-286, Aug. 2005.
[29] Standley, S. P., "Cassini–Huygens Engineering Operations at Saturn," AIAA Paper 2006-5516, June 2006.
[30] Wagner, S., Gist, E. M., Goodson, T. D., Hahn, Y., Stumpf, P. W., and Williams, P. N., "Cassini–Huygens Maneuver Experience: Second Year of Saturn Tour," AIAA Paper 2006-6663, Aug. 2006.
[31] Strange, N. J., and Sims, J. A., "Methods for the Design of V-Infinity Leveraging Maneuvers," American Astronautical Society Paper 01-437, July/Aug. 2001.
[32] Strange, N. J., "Control of Node Crossings in Saturnian Gravity-Assist Tours," American Astronautical Society Paper 03-545, Aug. 2003.
[33] Strange, N. J., Russell, R. P., and Buffington, B. B., "Mapping the V-Infinity Globe," American Astronautical Society Paper 07-277, Aug. 2007.
[34] Broucke, R. A., "The Celestial Mechanics of Gravity Assist," AIAA Paper 1988-4220, Aug. 1988.
[35] Cesarone, R. J., "A Gravity Assist Primer," *AIAA Student Journal*, Vol. 27, Spring 1989, pp. 16–22.
[36] Beckman, J. C., and Smith, D. B., "The Jupiter Orbiter Satellite Tour Mission," American Astronautical Society Paper 73-231, July 1973.
[37] Roy, A. E., *Orbital Motion*, 2nd ed., Adam Hilger, Bristol, England, UK, 1982, pp. 129–130.
[38] Labunsky, A. V., Papkov, O. V., and Sukhanov, K. G., *Multiple Gravity Assist Interplanetary Trajectories*, 1st ed., Gordon and Breach, Amsterdam, 1998, pp. 101–197.
[39] Strange, N. J., and Longuski, J. M., "Graphical Method for Gravity-Assist Tour Design," *Journal of Spacecraft and Rockets*, Vol. 39, No. 1, 2002, pp. 9–16. doi:10.2514/2.3800
[40] Heaton, A. F., Strange, N. J., Longuski, J. M., and Bonfiglio, E. P., "Automated Design of the Europa Orbiter Tour," *Journal of Spacecraft and Rockets*, Vol. 39, No. 1, 2002, pp. 17–22. doi:10.2514/2.3801
[41] Kizner, W., "A Method of Describing Miss Distances for Lunar and Interplanetary Trajectories," Jet Propulsion Lab., California Inst. of Technology External Publication 674, Aug., 1959.
[42] Yamakawa, H., Kawaguchi, J., Ishil, N., and Matsuo, H., "On Earth-Moon Transfer Trajectory with Gravitational Capture," American Astronautical Society Paper 93-633, Aug. 1993.
[43] Howell, K. C., Grebow, D., and Olikara, Z., "Design Using Gauss' Perturbing Equations with Applications to Lunar South Pole Coverage," American Astronautical Society Paper 07-143, Jan. 2007.
[44] Villac, B., and Scheeres, D., "The Effect of Tidal Forces on Orbit Transfers," American Astronautical Society Paper 01-247, Feb. 2001.
[45] Rinderle, E. A., "Galileo User's Guide, Mission Design System, Satellite Tour Analysis and Design Subsystem," Jet Propulsion Lab., California Inst. of Technology Internal Document D-263, July 1986.
[46] Williams, S. N., "Automated Design of Multiple Encounter Gravity-Assist Trajectories," M.S. Thesis, School of Aeronautics and Astronautics, Purdue Univ., West Lafayette, IN, Aug. 1990.
[47] Longuski, J. M., and Williams, S. N., "Automated Design of Gravity-Assist Trajectories to Mars and the Outer Planets," *Celestial Mechanics and Dynamical Astronomy*, Vol. 52, No. 3, 1991, pp. 207–220. doi:10.1007/BF00048484
[48] Patel, M. R., "Automated Design of Delta-V Gravity-Assist Trajectories for Solar System Exploration," M. S. Thesis, School of Aeronautics and Astronautics, Purdue Univ., West Lafayette, IN, Aug. 1993.
[49] Bonfiglio, E. P., "Automated Design of Gravity-Assist and Aerogravity-Assist Trajectories," M. S. Thesis, School of Aeronautics and Astronautics, Purdue Univ., West Lafayette, IN, Aug. 1999.
[50] Howell, K. C., and Anderson, J., User's Guide: Purdue Software GENERATOR, School of Aeronautics and Astronautics, Purdue Univ., West Lafayette, IN, July 2001.
[51] Buffington, B., and Strange, N. J., "Patched-Integrated Gravity-Assist Trajectory Design," American Astronautical Society Paper 07-276, Aug. 2007.
[52] Russell, R. P., and Ocampo, C. A., "Global Search for Idealized Free-Return Earth-Mars Cyclers," *Journal of Guidance, Control, and*

Dynamics, Vol. 28, No. 2, 2005, pp. 194–208.
doi:10.2514/1.8696

[53] Byrnes, D. V., and Bright, L. E., "Design of High-Accuracy Multiple Flyby Trajectories Using Constrained Optimization," American Astronautical Society, AAS Paper 95-307, Aug. 1995.

[54] Russell, R. P., and Ocampo, C. A., "Geometric Analysis of Free-Return Trajectories Following a Gravity-Assisted Flyby," *Journal of Spacecraft and Rockets*, Vol. 42, No. 1, 2005, pp. 138–151.
doi:10.2514/1.5571

C. Kluever
Associate Editor